

# Solutions to Maxwell equations for an electromagnetic beam injected into a plasma

Yacine Benhadid

**Abstract.** Maxwell equations are solved in a two dimensional plasma sheet for the case of an electromagnetic beam (laser beam for example) entering the media. The main idea is to separate the wave as the sum of two waves: one propagating forward, the second backward. The boundary conditions are the vacuum field at the left boundary, zero at the right boundary. The left field not yet taken into account by these two waves are considered at first as part of a generalized current, and then solved, shifted in time by half a time step. The present paper deals with TM and TE cases. Numerical results are brought for both.

**M.S.C. 2000:** 65M06, 65M50, 65Z05, 78M25.

**Key words:** Maxwell equations, wave propagation, splitting technique.

## §1. Introduction

To understand the physical processes of charged particles behavior (electrons and/or ions) when a strong electromagnetic (EM) field (a laser beam for example) strikes a plasma, brings to study electromagnetic-plasma interaction.

This is done numerically with the help of particles (PIC) or Vlasov-Eulerian codes. Since high space dimension requires a great numerical effort because of the number of space points increasing with dimensionality, we restrain the problem to 2D space dependence. The first dimension is the direction of the beam in free space, the second dimension being perpendicular to the main propagation direction.

In the present work, we will study numerical solutions to the Maxwell equations for the case of a beam striking a 2D plasma sheet surrounded by void space.

Since the pioneering work by K.C.Yee ([11]), finite difference in space and time are widely used to obtain numerical solutions to Maxwell equations. These solutions are unstable due to waves reflection on the boundaries and to steepening of gradients in calculating space derivatives. To avoid these problems some authors propose to introduce artificial boundary layers ([6, 1, 2]). In the present work since most of the wave energy propagates in the initial beam direction, we choose to solve the problem as a forward/backward wave propagation (that problem can be solved direct integration along characteristics), the other components of the wave being solved again by integration along characteristics at an intermediate time step.

## §2. Maxwell equations

Electromagnetic phenomena in a domain  $\Omega \subset \mathcal{R}^3$  occupied by a medium and all time of  $\mathcal{R}$  (or only for positive  $t$  or for a finite interval of time  $\mathcal{R}_t$ ) are described in plasmas by the two functions  $E$  and  $B$  of  $(X, t) \in \Omega \times \mathcal{R}_t$  with values in  $\mathcal{R}^3$  where  $E$  is the electric field and  $B$  the magnetic induction. The free charges  $\rho$  and currents  $J$  are calculated by the plasma (PIC or Vlasov-Eulerian) codes.

These functions are related by the Maxwell equations (2.1) where units are chosen so that the speed of light is 1:

$$(2.1) \quad \left\{ \begin{array}{ll} \text{i) } \frac{\partial}{\partial t}(E) - \text{curl } B = -J & \text{Ampere's law,} \\ \text{ii) } \frac{\partial B}{\partial t} + \text{curl } E = 0 & \text{Faraday's law,} \\ \text{iii) } \text{div } E = \frac{1}{\epsilon_0} \rho & \text{Poisson equation,} \\ \text{iv) } \text{div } B = 0 & \text{Gauss magnetic law.} \end{array} \right.$$

where  $\epsilon_0$  is the permittivity of the plasma.

We use the notations *div* and *curl*, which in the 2D case take the form for a Cartesian system of coordinates:

$$(2.2) \quad \text{div} E = \frac{\partial E_x}{\partial x} + \frac{\partial E_y}{\partial y} + \frac{\partial E_z}{\partial z},$$

$$(2.3) \quad \text{curl} E = \left( \frac{\partial E_z}{\partial y} - \frac{\partial E_y}{\partial z}, \frac{\partial E_x}{\partial z} - \frac{\partial E_z}{\partial x}, \frac{\partial E_y}{\partial x} - \frac{\partial E_x}{\partial y} \right).$$

The current density and the free charges satisfy the continuity relation of charge conservation law:

$$(2.4) \quad \frac{\partial \rho}{\partial t} + \text{div} J = 0,$$

which is the equation of total charge conservation.

Taking the divergence of Ampere's and Faraday's laws, it is an immediate conclusion that Gauss's magnetic law and Poisson's equation are fulfilled if we assume at initial time that

$$(2.5) \quad \text{div} B_{(t=0)} = 0,$$

and

$$(2.6) \quad \text{div} E_{(t=0)} = \rho_{(t=0)} / \epsilon_0.$$

Taking into account the conditions (2.5) and (2.6), we can deal from now on only with Faraday's and Ampere's equations (1.ii) and (1.i). From equation (1.iv), it is obvious that the magnetic induction  $B$  ensues from a vector potential  $A(x, y, t)$

$$(2.7) \quad B = \nabla \times A \quad (B = \text{curl} A),$$

and from equations (2.1.ii) and (2.1.iii) that the electric field  $E$  has two parts, one following from a scalar potential  $\Phi(x, y, t)$  and the second from the vector potential  $A(x, y, t)$

$$(2.8) \quad E = -\nabla\Phi - \frac{1}{c} \frac{\partial A}{\partial t},$$

where  $c$  is the speed of light.

### §3. Resolution of Maxwell equations

It is well known that we can decompose any electromagnetic field into "transverse electric" and "transverse magnetic" fields ([11]).

The two modes are characterized by

1. Transverse magnetic wave (TM)

$$(3.9) \quad \vec{A} = (0, 0, A_z) \Rightarrow E_x = E_y = 0, B_z = 0$$

so that in this case Maxwell equations become

$$(3.10) \quad \begin{cases} \frac{\partial E_z}{\partial t} + \frac{\partial B_x}{\partial y} - \frac{\partial B_y}{\partial x} = -J_z, \\ \frac{\partial B_x}{\partial t} + \frac{\partial E_z}{\partial y} = 0, \\ \frac{\partial B_y}{\partial t} - \frac{\partial E_z}{\partial x} = 0. \end{cases}$$

and

2. Transverse electric wave (TE)

$$(3.11) \quad \vec{A} = (A_x, A_y, 0) \Rightarrow B_x = B_y = 0, E_z = 0$$

$$(3.12) \quad \begin{cases} \frac{\partial E_x}{\partial t} = \frac{\partial B_z}{\partial y} - J_x, \\ \frac{\partial E_y}{\partial t} = -\frac{\partial B_z}{\partial x} - J_y, \\ \frac{\partial B_z}{\partial t} = -\frac{\partial E_y}{\partial x} + \frac{\partial E_x}{\partial y}. \end{cases}$$

Since we are dealing with the propagation of a beam propagating principally in the  $x$  direction, we seek for a solution similar to the 1D case (e.g., [4]), where the wave can be solved with a high degree of precision, solving for a propagating and a reflected wave in the  $x$  direction.

At the beginning, we shall start with the TM wave. In this case,  $E_z$  field is strongly perturbed by spurious reflection effects with  $y$  boundaries even in periodic case. To solve the problem, we split the  $E_z$  field into  $E_{zx}, E_{zy}$ , following [1],[9]. To

damp these spurious waves, we also introduce electric and magnetic conductivities in the  $y$  direction  $\sigma_y$  and  $\sigma_y^*$ . Introducing this splitting and damping into the Ampere's and Faraday's equations gives

$$(3.13) \quad \begin{cases} \frac{\partial E_{zx}}{\partial t} = \frac{\partial B_y}{\partial x}, \\ \frac{\partial E_{zy}}{\partial t} + \sigma_y E_{zy} = \frac{\partial B_x}{\partial y} - J_z, \\ \frac{\partial B_x}{\partial t} + \sigma_y^* B_x = -\frac{\partial(E_{zx} + E_{zy})}{\partial y}, \\ \frac{\partial B_y}{\partial t} = \frac{\partial(E_{zx} + E_{zy})}{\partial x}. \end{cases}$$

For the resolution of this system, we proceed at first to solve the two equations with the damping conductivity according that

$$(3.14) \quad \sigma_y = \sigma_y^* = \sigma$$

then we solve the others without damping.

The system (3.13) becomes:

$$(3.15) \quad \begin{cases} \frac{\partial E_{zy}}{\partial t} + \sigma E_{zy} = \left( \frac{\partial B_x}{\partial y} - J_z \right), \\ \frac{\partial B_x}{\partial t} + \sigma B_x = -\frac{\partial(E_{zx} + E_{zy})}{\partial y}, \end{cases}$$

$$(3.16) \quad \begin{cases} \frac{\partial E_{zx}}{\partial t} = \frac{\partial B_y}{\partial x}, \\ \frac{\partial B_y}{\partial t} = \frac{\partial(E_{zx} + E_{zy})}{\partial x}. \end{cases}$$

The system (3.16) can be solved as a sum of forward and backward propagating waves

$$(3.17) \quad \begin{cases} E^+ = E_{zx} + B_y, \\ E^- = E_{zx} - B_y, \end{cases}$$

The system (3.16) reduces to (3.18), the right handside which defines a new current to be called  $g_1$

$$(3.18) \quad \left( \frac{\partial}{\partial t} \mp \frac{\partial}{\partial x} \right) E^\pm = -\frac{\partial E_{zx}}{\partial x} = g_1,$$

with boundary conditions  $E^+(x=0) = E^+$  value of the incoming wave, and  $E^-(x=L) = 0$ , since there are no reflected waves from outside the plasma. (3.18) is solved iteratively with a time step  $\Delta t$ ,  $g_1$  being calculated half a time step before (see appendix).

To resolve the system in (3.15), the  $E^\pm$  waves are now

$$(3.19) \quad \begin{cases} E^+ = E_{zy} + B_x, \\ E^- = E_{zy} - B_x. \end{cases}$$

and the system (3.15) takes the form (3.20), the right handside which defines a new current to be called  $g_2$ , also calculated half a time step before (3.20) is solved.

$$(3.20) \quad \left( \frac{\partial}{\partial t} \mp \frac{\partial}{\partial y} + \sigma \right) E^\pm = -\frac{\partial B_y}{\partial x} - J_z = g_2.$$

To solve (3.15), we introduce  $E_0^\pm$ , so that

$$(3.21) \quad E^\pm = E_0^\pm e^{\pm \sigma y}.$$

The system (3.15) reduces to:

$$(3.22) \quad \left[ \left( \frac{\partial}{\partial t} \mp \frac{\partial}{\partial y} \right) E_0^\pm \right] e^{\pm \sigma y} = g_2,$$

or

$$(3.23) \quad \left( \frac{\partial}{\partial t} \mp \frac{\partial}{\partial y} \right) E_0^\pm = g_2 e^{\mp \sigma y}.$$

The boundary conditions are  $E^+(y = y_{max}) = 0$  and  $E^-(y = y_{min}) = 0$ , since no reflected waves from outside the plasma exist.

The TM and TE are in some way similar. So as in TM, in the transverse electric case, the electromagnetic field reduces to four components  $E_x$ ,  $E_y$ ,  $B_{zx}$ ,  $B_{zy}$  where here  $B_z$  is the field which is splitted into two subcomponents. Again, we damp the spurious waves by introducing the conductivity  $\sigma$ . Then our system becomes:

$$(3.24) \quad \begin{cases} \frac{\partial E_x}{\partial t} + \sigma E_x = \left( \frac{\partial(B_{zx} + B_{zy})}{\partial y} - J_x \right), \\ \frac{\partial B_{zy}}{\partial t} + \sigma B_{zy} = \frac{\partial E_x}{\partial y}, \end{cases}$$

$$(3.25) \quad \begin{cases} \frac{\partial E_y}{\partial t} = -\frac{\partial(B_{zx} + B_{zy})}{\partial x} - J_y, \\ \frac{\partial B_{zx}}{\partial t} = -\frac{\partial E_y}{\partial x}. \end{cases}$$

As in the TM case, the system (3.25) can be solved as a sum of forward and backward propagating waves

$$(3.26) \quad \begin{cases} E^+ = E_y + B_{zx}, \\ E^- = E_y - B_{zx}. \end{cases}$$

The system (3.25) reduces to ( $g_1$  is as in the TM case a new current):

$$(3.27) \quad \left( \frac{\partial}{\partial t} \mp \frac{\partial}{\partial x} \right) E^\pm = -\frac{\partial B_{zy}}{\partial x} - J_y = g_1,$$

To resolve the system (3.24), the  $E^\pm$  waves are now

$$(3.28) \quad \begin{cases} E^+ = E_x + B_{zy}, \\ E^- = E_x - B_{zy}, \end{cases}$$

and with introducing  $E_0$ , the system (3.24) takes the form (3.29) with  $g_2$  a new current as in the TM case:

$$(3.29) \quad \left( \frac{\partial}{\partial t} \mp \frac{\partial}{\partial x} \right) E_0^\pm = \frac{\partial B_{zx}}{\partial y} - J_x = g_2.$$

At the end, we see that in each case (TM and TE), we have to solve an inhomogeneous transport equation which done using the numerical method shown later in the appendix.

#### §4. Numerical results

We present in this section numerical results of electromagnetic waves propagation, in TM and TE modes.

We start again with the TM mode. First we solve the 1-dimensional wave equation in  $x$  direction for  $E_z$  and  $B_y$ ,  $E_z$  being calculated from

$$(4.30) \quad \frac{\partial B_x}{\partial t} = -\frac{\partial E_z}{\partial y}$$

by finite differences. The results presented in figure 1 is for an initial signal with a  $\sin(\alpha y)$  shape. The numerical derivatives make the  $y$  profile sharper and sharper as the number of iteration increase, and noisy. The result after 60 iterations is given fig. 1. To avoid these kind of effects, we have used the idea of splitting  $E_z$  in two parts, one propagation in  $x$  direction, the second in  $y$  direction. The latter method brings to solve four waves two in  $x$  and two in  $y$ . To test the method, we start with an initial pulse of sinus form in time ( $E_{zx}(x=0) = 0.5\cos(\omega t)$ ,  $B_y(x=0) = 0.5\sin(\omega t)$ ,  $\omega = 6\pi$ ,  $t$  varying from zero to  $1/\omega$ ,  $E_{zx}$  and  $B_y(x=0, t)1/\omega$  are null). The profile is homogenous in  $y$  direction. The wave propagates without any perturbation see fig. 2. The propagation of waves with the same initial condition for the entering wave, and the profile described for fig. 1 is shown in fig. 3. In the latter case a small current is present constant in time of the form:

$$(4.31) \quad J_z = \frac{1}{10}\sin(x) * \cos(\pi y).$$

The damping coefficient  $\sigma$  is null in the results presented fig. 3. In the display of the  $E_{zy}$  field, an  $X$  shape signal coming from spurious non damped waves entering the system are present. In the  $B_x$  figure, the same signature exists, but we see also a propagating wave, generated by the wave dispersion, due to the  $y$  shape of the entering wave.

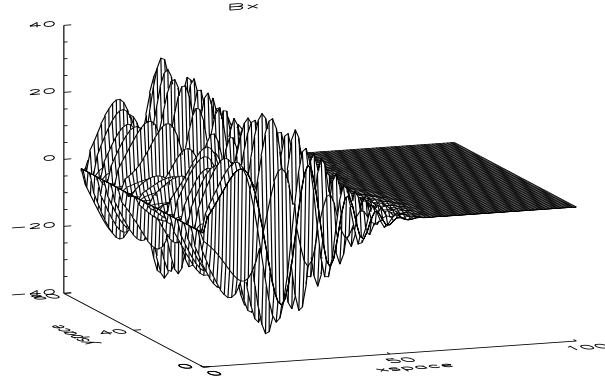


Figure 1: The  $B_x$  field after 50 iterations, computed by finite differences.

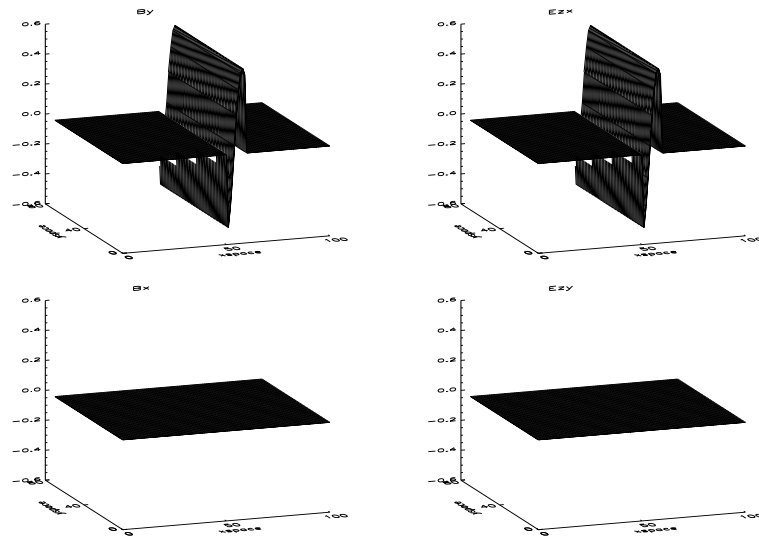


Figure 2: TM wave propagation. Homogeneous  $y$  profile, no current.  $B_y$ ,  $E_z$ ,  $B_x$ ,  $E_y$  versus position after 60 iterations.

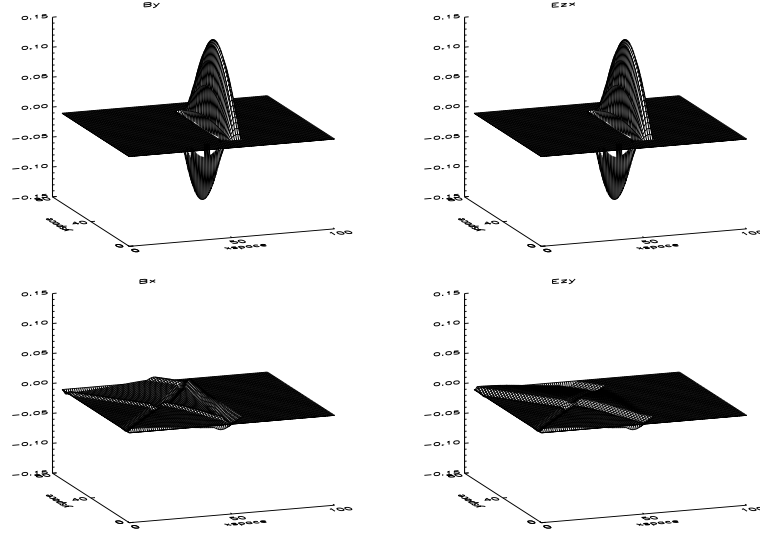


Figure 3: *TM wave propagation. Homogeneous y profile, no current.  $B_y$ ,  $E_{zx}$ ,  $B_x$ ,  $E_{zy}$  versus position after 60 iterations.*

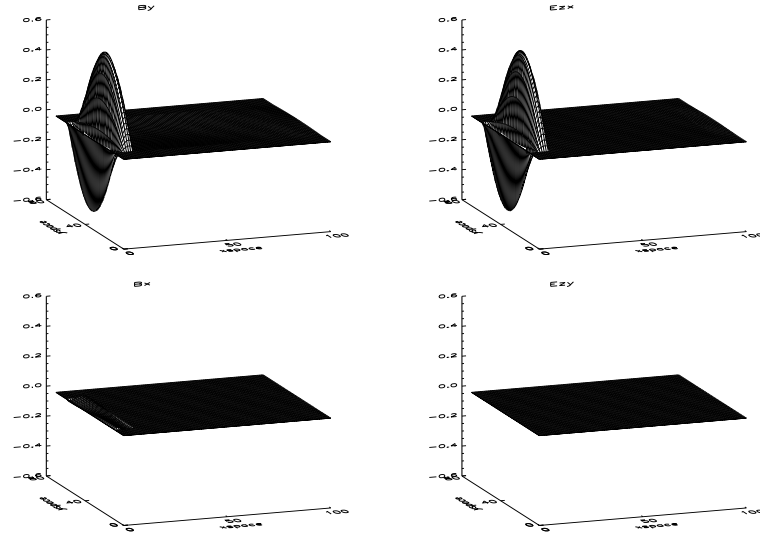


Figure 4: *The TM waves after 10 iterations. The whole initial pulse is now in the computational box.*



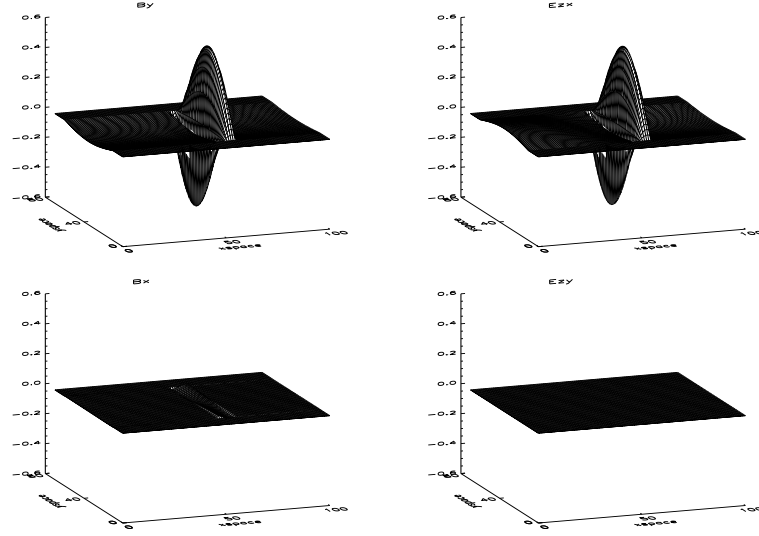


Figure 5: *The TM waves after 100 iterations. The signal is now exciting the computational box.*

Introducing a non null  $\sigma$  factor damps the spurious effects and the effect coming from the wave dispersion is clearly shown (fig. 4 and 5). The Transverse Electric case is calculated in a way similar to that presented for the TM case. Now the entering waves are  $E_y$  and  $B_{zx}$ . In vacuum  $E_x$  and  $B_{zy}$  are null.

As expected, an entering wave without an  $y$  shape propagates without change along the computational box. No  $E_x$  and  $B_{zy}$  fields are created by fallacious numerical effects. These results are presented fig. 6. Figures 7 and 8 show the propagation of a wave with an initial  $y$  shape of the sine type similar to the one used for the TM wave - a half cosine centered around the mean  $y$  value, with zero values near  $y$  boundaries.

The last simulation presented here (fig. 9 and 10) is for the same entering wave as in figures 7 and 8 but now we have introduced a strong electric current, constant in time of the form:

$$(4.32) \quad \begin{cases} J_x = -\frac{1}{2} \sin x * \cos(\pi y), \\ J_y = \frac{1}{10} \sin x * \sin y. \end{cases}$$

for  $0 < x < L$  and  $y_{min} < y < y_{max}$ .

This generates a small  $E_x$  field, constant in time as the current. The  $E_x$  field includes also a propagating part generated by the dispersion effect.

## §5. Conclusions

We have shown in the present paper an efficient numerical method to solve Maxwell equations for a pulse entering a two dimensional sheet. Both cases of TM and TE

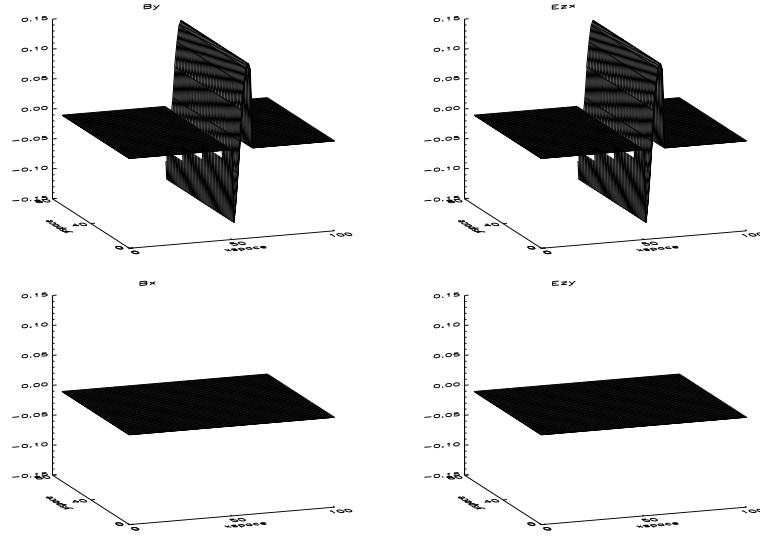


Figure 6: *TE wave propagation. Homogeneous y shape.*

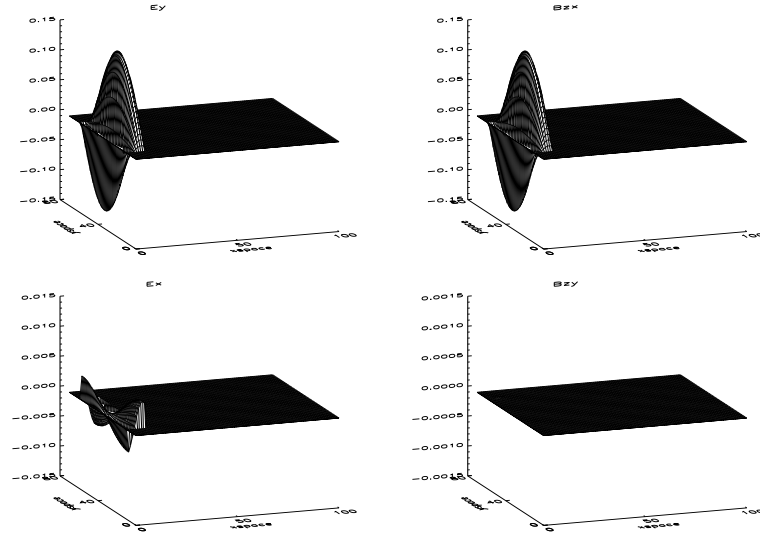


Figure 7: *TE wave propagation. The wave after entering the computational box.*

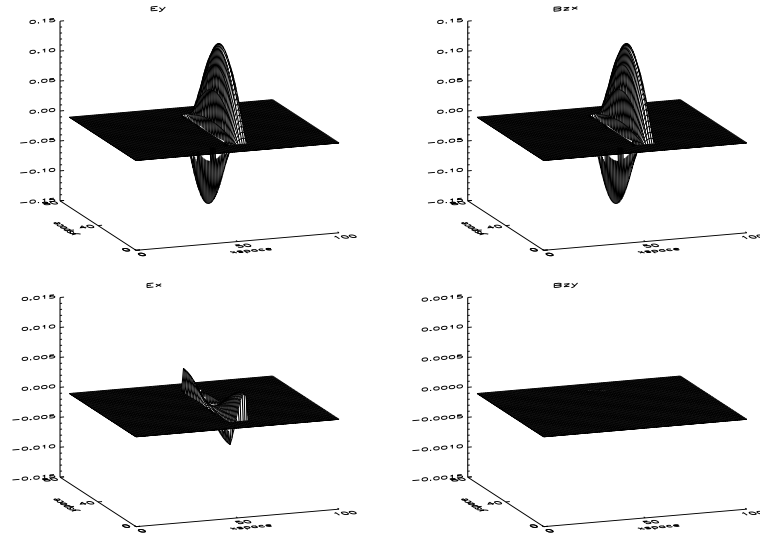


Figure 8: *TE wave with a cosine y shape propagation. After 60 iterations.*

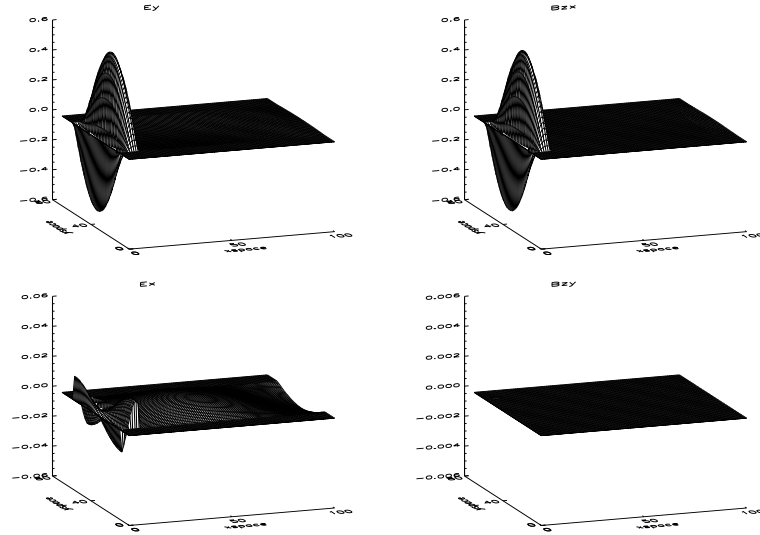


Figure 9: *E wave propagation with a constant current. The entering field and the  $E_x$  field generated by the current.*

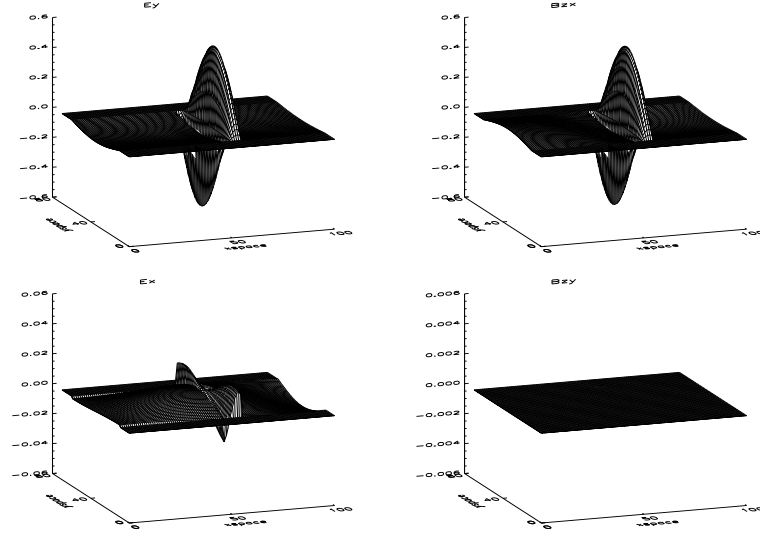


Figure 10: *TE wave, y shape, current, after 60 iterations.*

waves are treated. To summarize the method, one of the waves (the  $E_z$  wave for TM, the  $B_z$  for TE) is splitted into two parts, one propagating along the direction of the entering wave, the second perpendicular to it. Then the system is solved as the sum of two propagating forward and backward waves in  $x$  direction, and the same for the perpendicular direction. The propagation is then calculated along the characteristics. The proposed method avoids the problems generated by numerical calculations of space derivatives. The method also allows not to use damping factors in the main propagation direction, presenting a good method to be used for Vlasov-Maxwell problems in the case of beam-plasma interaction.

## §6. Appendix

Let us observe the homogeneous transport equation:

$$(6.33) \quad \left( \frac{\partial}{\partial t} \mp \frac{\partial}{\partial x} \right) E^{\pm} = 0$$

For example, if we use the standard 3-point central finite differences approximation, we obtain

$$(6.34) \quad \frac{\partial E_n^{\pm}}{\partial t} = \frac{E_{n+1}^{\pm} - E_{n-1}^{\pm}}{2\Delta x} \quad n = \dots, -1, 0, 1, \dots$$

Such a system of difference-differential equations is called a semi-discretization of the partial differential equation. We introduce the space shift operator  $F$ ., defined by the relation

$$(6.35) \quad E_{n+1} = F.E_n \quad \text{or} \quad E_{n-k} = F(k).E_n,$$

which is read as "the operator  $F$ . to the k-th power". Then, we may rewrite the preceding approximation in symbolic notation as

$$(6.36) \quad \frac{\partial E_n}{\partial t} = A.E_n,$$

where  $A$ . is the operator

$$(6.37) \quad A. = - \left( \frac{F. - F.^{-1}}{2\Delta x} \right)$$

We proceed now to a full discretization of the equation, for that, we apply on the semi-discretization a time marching method for the ordinary differential equation. To obtain more stability of the numerical scheme, we must change our standard 3-point central semi-discretization by another implicit 2-point semi-discretization ("in box")

$$(6.38) \quad \frac{1}{2} \left( \frac{\partial E_n^+}{\partial t} + \frac{\partial E_{n+1}^+}{\partial t} \right) = \frac{E_{n+1}^+ - E_n^+}{\Delta x}$$

Then we get

$$(6.39) \quad \frac{1}{2}(1 - F.) \frac{\partial E_n^+}{\partial t} = \left( \frac{F. - 1}{\Delta x} \right) E_n^+$$

In operator mode (6.39) becomes

$$(6.40) \quad A_1. \frac{\partial E_n^+}{\partial t} = A_2. E_n^+$$

where  $A_1. = \frac{1}{2}(1 - F.)$  and  $A_2. = \frac{F.-1}{\Delta x}$ . We define the function  $\hat{A}$  as

$$(6.41) \quad \hat{A}(\omega) = \frac{A_1.e^{i\omega x_n}}{A_2.e^{i\omega x_n}}.$$

$\hat{A}(\omega)$  is called the spectral function of the operator  $A$  ( $\hat{A}$  correspond to the eigenvalues of  $A$ ). We say that a numerical method is conservative when  $Re\hat{A}(\omega) = 0$ . In this case, the only discrepancy between numerical sinusoidal solutions and their exact counterparts is in the velocity at which they propagate. We define the function

$$(6.42) \quad c^*(\omega) = \frac{-Im\hat{A}(\omega)}{\omega}.$$

$c^*(\omega)$  is the velocity of propagation of numerical sinusoidal.  $c^*(\omega)$  is called the phase velocity. Returning to our semi-discretization, we define the spectral function  $\hat{A}(\omega)$  and the phase velocity  $c^*(\omega)$  of the numerical method.

$$(6.43) \quad \hat{A}(\omega) = -i \frac{\tan(\omega\Delta x/2)}{\omega\Delta x/2}$$

resulting in

$$(6.44) \quad c^*(\omega) = \frac{\tan(\omega\Delta x/2)}{\omega\Delta x/2}$$

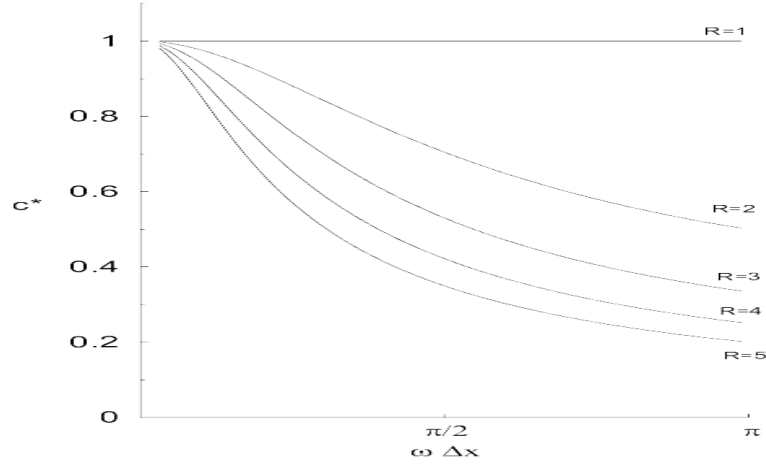


Figure 11: Numerical phase velocity of the "box method". Note the accuracy when  $R = 1$ . When  $R > 1$ , errors due to the approximation in space and in time directions are of the same sign, and are therefore additive ( $x, v$ ).

Now, we make a full discretization by applying to (6.36) a General Implicit Method:

$$(6.45) \quad E^{j+1} = E^j + \frac{\Delta t}{2}(A.E^{j+1} + A.E^j)$$

where

$$(6.46) \quad A. = \left( \frac{F. + 1}{2} \right)^{-1} \left( \frac{F. - 1}{2} \right).$$

The condition of numerical stability for several common marching methods when applied to the hyperbolic full-discretization may be expressed as

$$(6.47) \quad \left| \frac{\Delta t}{\Delta x} \right| < S_I,$$

where  $S_I$  is the value of  $|\Delta t \hat{A}|$  at which the stability boundary  $S$  intersects the imaginary axis. The value of  $S_I$  for the General Implicit Method (with  $q = 1/2$  see [10]) is

$$(6.48) \quad S_I = +\infty \rightarrow \left| \frac{\Delta t}{\Delta x} \right| < +\infty.$$

We always have stability. In the same way, we find the phase velocity (see fig. 11)

$$(6.49) \quad c^*(\omega) = \frac{2 \arctan(R \tan(\omega \Delta x / 2))}{R \omega \Delta x}$$

We define  $V(\omega)$  as

$$(6.50) \quad V(\omega) = \frac{\partial}{\partial \omega}(\omega c^*(\omega)) = \frac{1 + \tan(\omega \Delta x/2)^2}{1 + R^2 \tan(\omega \Delta x/2)^2}.$$

$V(\omega)$  is called the group velocity.

It is important to note that the group velocity (or the velocity of the envelope) is a function of the modulating frequency  $\omega$ . We may also note that when the phase velocity is constant ( $c^*(\omega)=\text{constant}$ ), then it yields simply  $V = 1$ .

The theory of group velocity is important in the present context mainly explaining the propagation of short wavelength which appears near discontinuities in discrete approximations of hyperbolic equations. These spurious oscillations typically have a  $2\Delta x$  wavelength. Because of the nonconstancy of  $c^*(\omega)$ , the envelope of such spurious oscillations is observed to propagate at the group velocity  $V(p/\Delta x)$  rather than the phase velocity  $c^*(p/\Delta x)$ .

## References

- [1] J.P. Berenger, *A perfectly matched layer for the absorption of the electromagnetic waves*, J. Comp. Physics 114 (1994), 185-200.
- [2] J.P. Berenger, *Three-dimensional perfectly matched layer for the absorption of electromagnetic waves*, J. Comp. Physics, 127 (1996), 363-379.
- [3] M. Cessenat, *Mathematical Methods in Electromagnetism*, World Scientific, 1996.
- [4] A.J. Chorin, J.E. Marsden, *A Mathematical Introduction to Fluids Mechanics*, Springer Verlag, 1979.
- [5] E. Godlewski, P.A. Raviart, *Numerical approximation of hyperbolic systems of conservation laws*, Springer Verlag, 1996.
- [6] R. Holland, J.W. Williams, *Total-field versus scattered-field finite difference codes: a comparative assessment*, IEEE Trans. 30 (1983), 4583-4588.
- [7] L.D. Landau, E.M. Lifshitz, *The Classical Theory of Fields*, Pergamon Press, 1962.
- [8] M.E. Taylor, *Partial Differential Equations I*, Springer Verlag, 1996.
- [9] J.L. Vay, *A New FDTD Scheme for the Wave Equation. Application to Multiscale Electromagnetic Plasma Simulation*, 16-th International Conference on Numerical Simulation of Plasma Proceedings, Santa Barbara, Springer Verlag 1998, 270-283.
- [10] R. Vichnevetsky, J.B. Bowles, *Fourier Analysis of Numerical Approximations of Hyperbolic Equations*, SIAM, 1982.
- [11] K.S. Yee, *Numerical solution of initial boundary value problems involving Maxwell's equation in isotropic media*, IEEE Trans. Antennas Propagation 14 (1966), 302-320.

*Author's address:*

Yacine Benhadid  
 College of Science, Department of Mathematics, P.O. Box 2455,  
 Riyadh 11451, Saudi Arabia.  
 e-mail: benhadid@ksu.edu.sa